Nanoscale Research Letters

NANO EXPRESS Open Access

$Cu_{2-x}Se$ Modification onto Monoclinic $BiVO_4$ for Enhanced Photocatalytic Activity Under Visible Light

Zirui Liu[1], Xiaoyong Liu[2*], Xinxin Gu[3], Renqing Guo[3] and Wenwu Zhong[3*]

Abstract

The rapid recombination of electron-hole pairs in $BiVO_4$ has limited its performance as a photocatalysis. In this paper, $BiVO_4$ is combined with $Cu_{2-x}Se$ semiconductor to slow down the recombination process, and thus improve its photocatalytic activity. This is enabled by careful band structure design. The work function of $Cu_{2-x}Se$ is larger than that of $BiVO_4$. Therefore, electrons flow to $Cu_{2-x}Se$ from $BiVO_4$ after the composition. Accordingly, an inner field could be built, which facilitates the separation of electrons and holes. The experimental result shows that the photocatalytic efficiency of the 3 wt% $Cu_{2-x}Se/BiVO_4$ composite is 15.8 times than that of pure $BiVO_4$.

Keywords: Photocatalysis, Hydrothermal, Bismuth-based semiconductor

Introduction

With the developing of modern industry, environmental pollution has become more and more severe. Utilizing solar energy, photocatalytic decomposition of organic matter is an environmentally friendly and efficient technology to solve pollution [1–6]. The Bi-based semiconductor photocatalytic material has a suitable band gap, which enables it to absorb visible light sufficiently and possess superior photocatalytic performance [7–10]. Among them, monoclinic $BiVO_4$ has a narrow band gap of 2.4 eV and good photocatalytic activity, which has been nominated as an efficient material for decomposing organic pollutions [11–15]. The rapid electron-hole recombination rate, however, leads to a low photocatalytic activity for pure $BiVO_4$ [16–18]. An effective approach to slow down the recombination of electrons and holes is to combine two different semiconductor materials, given the band structures of the two combined materials match a specific condition.

As a p-type semiconductor, Cu_{2-x} Se has an indirect bandgap of 1.4 eV, which is beneficial to absorb visible light [19–21]. When $BiVO_4$ semiconductor is compounded with $Cu_{2-x}Se$, redistribution of charges is caused. The work function of $Cu_{2-x}Se$ is larger than that of $BiVO_4$, and the Fermi energy is lower than that of $BiVO_4$ [22, 23]. Therefore, electrons flow to $Cu_{2-x}Se$ from $BiVO_4$ while holes flow the other way around. Accordingly, an inner field could be built pointing from $BiVO_4$ to $Cu_{2-x}Se$, which facilitates the separation of electrons and holes. When under illumination, the photo-generated electrons in $BiVO_4$ and photo-generated holes in $Cu_{2-x}Se$ will recombine preferentially, due to the band bending and inner field, leaving useful holes in $BiVO_4$. The useful holes possess higher energy level, which can benefit the generation of •OH species. These •OH species can break down long chains of organic matter into small molecules. Hence, the $Cu_{2-x}Se/BiVO_4$ composites are expected to have high visible light photocatalytic activity.

In this work, we have fabricated Cu_{2-x} Se/$BiVO_4$ composites and made use of it for the degradation of RhB under visible light irradiation (> 420 nm) for the first time. After compounding with Cu_{2-x} Se, the photocatalytic activity becomes much higher than pure $BiVO_4$. Specifically, the photocatalytic efficiency of 3 wt% $Cu_{2-x}Se/BiVO_4$ composite is 15.8 times that of pure $BiVO_4$. Furthermore, after adding low concentration H_2O_2 into the organic solution, RhB completely degraded within 50 min. This work provides evidence that $Cu_{2-x}Se$ is an effective co-catalysis

* Correspondence: xyliu1983@cqu.edu.cn; tianmenwenwu@163.com
[2]School of Material Science and Engineering, Chongqing University, Chongqing 400044, China
[3]Department of Materials, Taizhou University, Taizhou 318000, China
Full list of author information is available at the end of the article

for the development of new composite semiconductor photocatalysts.

Methods

Preparation of $Cu_{2-x}Se/BiVO_4$ Composites

$BiVO_4$ was synthesized through a chemical precipitation method [24, 25]. The preparation method of $Cu_{2-x}Se$ can be found in our previously reported paper [26]. Then $Cu_{2-x}Se/BiVO_4$ composites were fabricated by a co-precipitation approach. The schematic illustration of the preparation progress is shown in Fig. 1. Firstly, the pre-prepared $Cu_{2-x}Se$ and $BiVO_4$ powders were dispersed in ethanol with constant stirring for 4 h under 60 °C. Secondly, the suspension of the mixture was continuously stirred at 80 °C to remove the ethanol solvent. Finally, the obtained powdery sample was heated at 160 °C for 6 h under a flowing nitrogen atmosphere to form the $Cu_{2-x}Se/BiVO_4$ composite.

Characterization

XRD (X-ray diffraction) measurement of the as-prepared samples was performed by a PANalytical X'pert Pro diffractometer with Cu Kα radiation. The morphology of the sample was obtained by an SEM (scanning electron microscope) Hitachi S-4800. XPS (X-ray photoelectron spectroscopy) of the samples was characterized on a Pekin Elmer PHI-5300 instrument. The photoluminescence emission spectra of the samples were committed using a Cary Eclipse fluorescence spectrophotometer.

Photocatalytic Reaction

The photocatalytic performance was characterized by an XPA photochemical reactor. Additionally, a Xe lamp with a power of 500 W and a cut-off wavelength of 420 nm is utilized to simulate natural light, while a solution of test dye RhB is used to mimic organic solutions. During the degradation process, 60 mg $Cu_{2-x}Se$ composite powder was placed in a 60-mL RhB solution. The suspension was stirred in a dark environment for 2 h before light irradiation to realize an adsorption-desorption balance. Then, light illumination is added with stirring remaining and about 6 mL of the suspension was taken out at intervals of 10 min. Subsequently, the suspension was centrifuged twice. The absorbance spectrum of the solution was characterized on a Shimadzu UV-2450 spectrometer.

Photoelectrochemical Measurements

The photocurrent is measured by a CHI 660E electrochemical workstation. To make the illumination consistent with that in the degradation process, the light source is still selected as a Xe lamp with a power of 500 W and a cut-off wavelength of 420 nm. The photoelectrochemical measurement is detailed as follows. First, 10 mg of the photocatalyst and 20 μL of Nafion solution were ultrasonically dispersed in 2 mL of ethyl alcohol. Then, 40 μL of the above solution was deposited on an ITO conductive glass with 0.196 cm^2, which was sequentially heated at 200 °C for 1 h to obtain the working electrode. Besides, Pt foil is chosen as the counter electrode. A saturated solution of mercury and mercurous chloride in an aqueous solution of potassium chloride as the reference electrode, and 0 .5M Na_2SO_4 solution is used for the electrolyte.

Results and Discussion

We used photodegradation of RhB to examine the photocatalytic properties of the samples. Figure 2a shows the photocatalytic degradation of RhB over $Cu_{2-x}Se/BiVO_4$. When $BiVO_4$ is combined with $Cu_{2-x}Se$, its photocatalytic performance is significantly improved. The optimum composite ratio is 3%, and the photocatalytic efficiency at this ratio reaches the maximum. Figure 2b shows the degradation rate of the $Cu_{2-x}Se/BiVO_4$ composites, corresponding

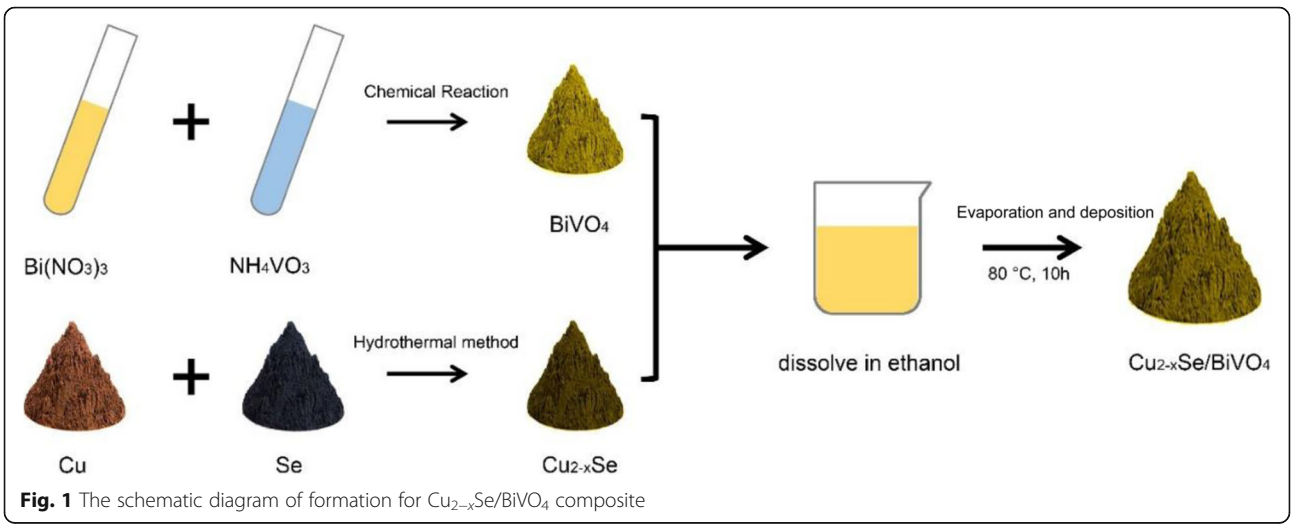

Fig. 1 The schematic diagram of formation for $Cu_{2-x}Se/BiVO_4$ composite

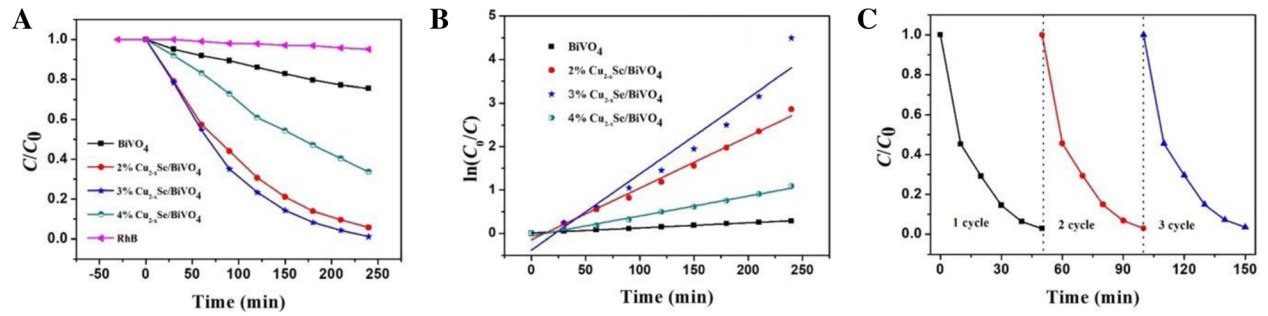

Fig. 2 **a** Photocatalytic degradation of RhB over $Cu_{2-x}Se/BiVO_4$. **b** Photocatalytic degradation rate constant of RhB for $Cu_{2-x}Se/BiVO_4$. **c** Recycle runs of photocatalytic degradation of RhB over 3 wt% $Cu_{2-x}Se/BiVO_4$ composite with H_2O_2 under visible light irradiation

to the concentration of $Cu_{2-x}Se$ with 0, 2, 3, and 4 wt%, respectively. In Fig. 2b, the slope value of degradation lines is 0.0011, 0.0118, 0.0174, and 0.0045 min^{-1}, respectively. Therefore, the photocatalytic efficiency of the 3 wt% $Cu_{2-x}Se/BiVO_4$ composite is 15.8 times than that of pure $BiVO_4$. Figure 2c shows the recycle runs of photocatalytic degradation of RhB over 3 wt% $Cu_{2-x}Se/BiVO_4$ composite with added H_2O_2 under visible light irradiation. When a small amount of H_2O_2 is added (103 μL/100 mL), the 3 wt% $Cu_{2-x}Se/BiVO_4$ composites can degrade RhB completely in 50 min under visible light excitation. It can also be seen from Fig. 2c that the degradation efficiency is not attenuated after 3 cycles.

In order to analyze the microscopic morphology and grain size of the samples, the samples were characterized by SEM. As shown in Fig. 3a, $BiVO_4$ is a hexagonal bulk with a particle size of 0.2–1 μm. In Fig. 3b, the area circled by the red solid line exhibits a $Cu_{2-x}Se$ sheet with a thickness of 300 nm and a length of 4 μm. After compounding, the $Cu_{2-x}Se$ sheets are randomly distributed on the surface of $BiVO_4$ bulk. The XPS results also reveal the presence of $Cu_{2-x}Se$ (shown below).

Figure 4a shows the XRD data for $BiVO_4$ and 3 wt% $Cu_{2-x}Se/BiVO_4$ composite, which exhibits that the $BiVO_4$ has a monoclinic crystal structure. It can be seen that the crystal structure of $BiVO_4$ does not change when $BiVO_4$ is combined with $Cu_{2-x}Se$. This may be due to the fact that the content of Cu is relatively too small to be detected by XRD. Photoluminescence measurement is a general way to explore the separation and combination of electrons and holes. The relatively low luminescence intensity means a high electron-hole separation efficiency [27, 28]. Figure 4b shows the PL spectra for $BiVO_4$ and $Cu_{2-x}Se/BiVO_4$ composites. After $BiVO_4$ is combined with $Cu_{2-x}Se$, the relative luminescence intensity of the $Cu_{2-x}Se/BiVO_4$ composite is lower than that of $BiVO_4$, which indicates that the $Cu_{2-x}Se/BiVO_4$ composite has higher electron-hole separation efficiency after the combination of $BiVO_4$ and $Cu_{2-x}Se$.

The surface chemical state plays an important role in determining photocatalytic performance. So XPS is used to analyze the surface element valence of the $Cu_{2-x}Se/BiVO_4$ composite. Figure 5a is the XPS survey spectrum of the $Cu_{2-x}Se/BiVO_4$ composite and pure $BiVO_4$, from

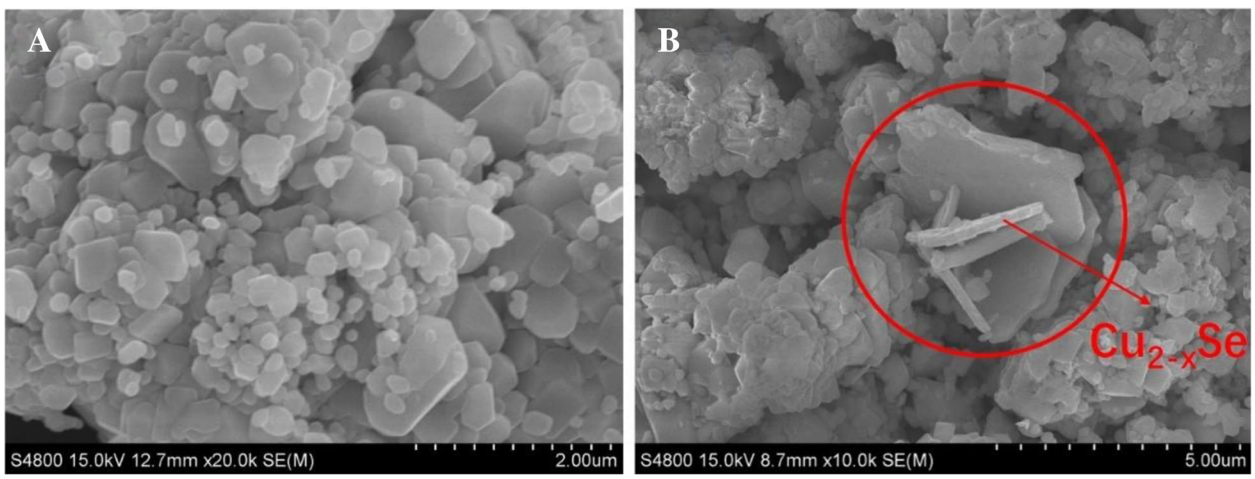

Fig. 3 The SEM photograph of $BiVO_4$ (**a**) and $Cu_{2-x}Se/BiVO_4$ (**b**)

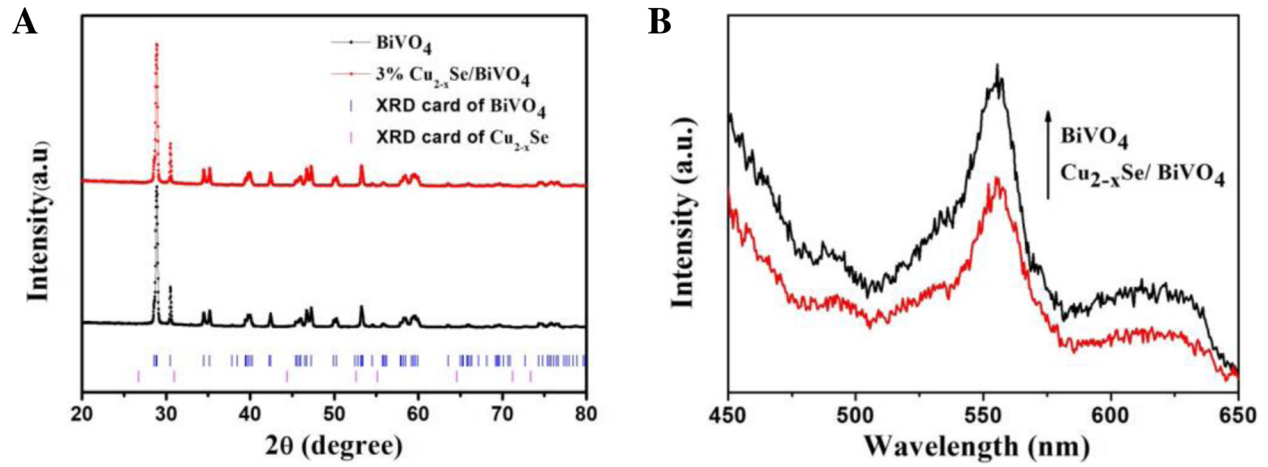

Fig. 4 The XRD data for $BiVO_4$ and 3% $Cu_{2-x}Se/BiVO_4$ (**a**), the PL spectra for $BiVO_4$ and $Cu_{2-x}Se/BiVO_4$ composites (**b**)

which characteristic energy of Bi, V, O, Cu, and Se can be observed for $Cu_{2-x}Se/BiVO_4$, and characteristic energy of Bi, V, and O can be observed for $BiVO_4$. The peaks of 159.1 and 164.1 eV can be attributed to the binding energies of Bi $4f_{7/2}$ and Bi $4f_{5/2}$, respectively (Fig. 5b), which are derived from Bi^{3+} in $BiVO_4$ [29]. The peaks of 517.0 eV and 525.0 eV correspond to V $2p_{3/2}$ and V $2p_{1/2}$ band respectively (Fig. 5c), which are derived from the V^{5+} of $BiVO_4$. The peak of 530.2 eV can be attributed to O 1 s in $BiVO_4$ (Fig. 5d) [30, 31]. The two peaks of 58.6 eV and 53.8 eV correspond to Se $3d_{3/2}$ and Se $3d_{5/2}$, respectively (Fig. 5e) [32]. The Cu $2p_{3/2}$ peak located at 931.9 eV corresponds to Cu^0 or Cu^I (Fig. 5f) [33].

To further illustrate the separation efficiency of photo-generated electrons and holes, the sample was subjected to EIS analysis. As shown in Fig. 6, the EIS Nyquist diagram of $Cu_{2-x}Se/BiVO_4$ has a smaller arc radius than $Cu_{2-x}Se$, indicating that $Cu_{2-x}Se/BiVO_4$ composites have smaller charge transfer resistance and faster interface electron transfer. [34, 35]

The reason why $Cu_{2-x}Se/BiVO_4$ composite exhibits high efficiency is explained as follows. As illustrated in Fig. 7, the Fermi level of $Cu_{2-x}Se$ and $BiVO_4$ disagrees

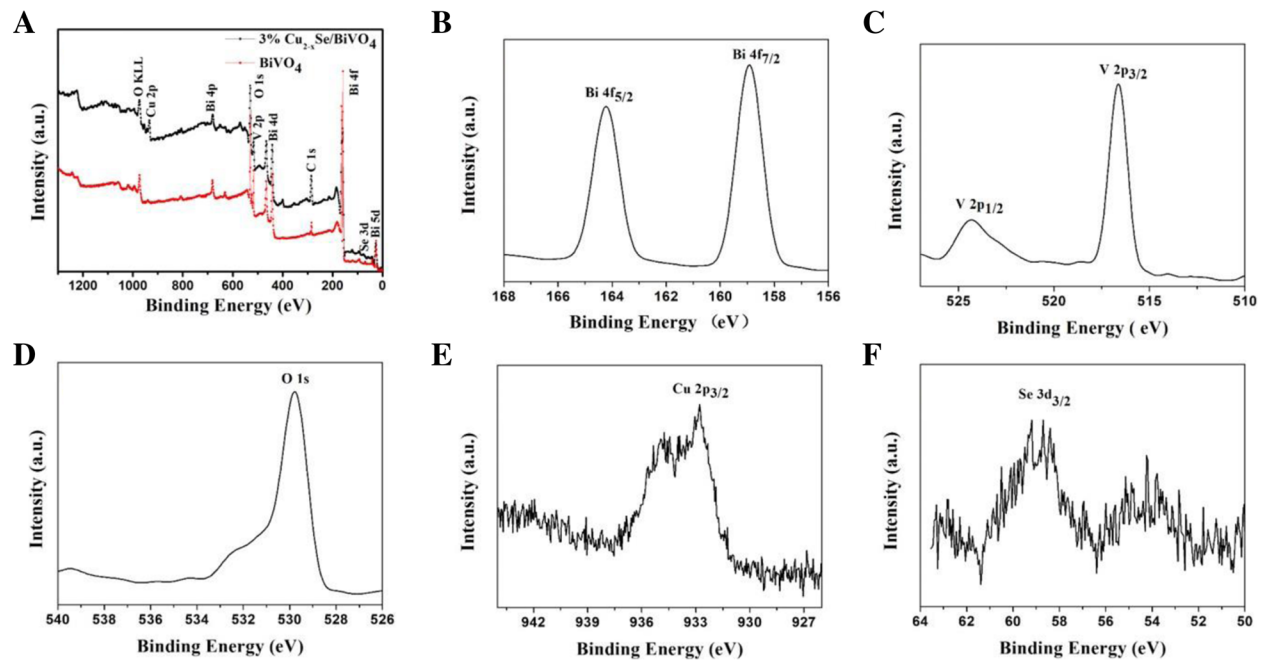

Fig. 5 The XPS spectra of $Cu_{2-x}Se/BiVO_4$ composite. **a** Survey, **b** Bi, **c** V, **d** O, **e** Cu, and **f** Se

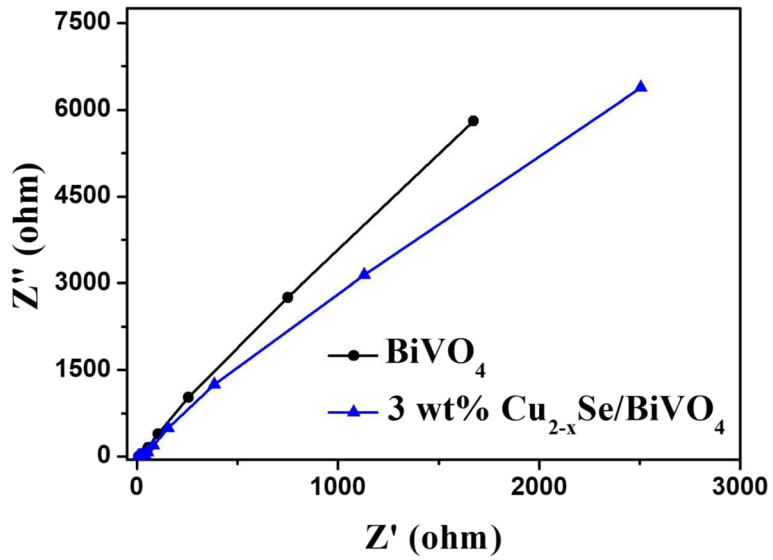

Fig. 6 The EIS for $BiVO_4$ and $Cu_{2-x}Se/BiVO_4$ under visible light irradiation in 0.5 M Na_2SO_4 solution

with each other. As a result, after the $BiVO_4$ semiconductor surface is compounded with CuSe, the charges will be redistributed. $Cu_{2-x}Se$ has larger work function and lower Fermi energy, so electrons flow to $Cu_{2-x}Se$ from $BiVO_4$ while holes flow the other way around. As a result, the $Cu_{2-x}Se$ is negatively charged and $BiVO_4$ is positively charged until the Fermi level is equal. Meanwhile, the band structure of both materials will bend corresponding to the movement of Fermi levels. Another effect of the redistribution of carriers is the building of an inner field pointing from $BiVO_4$ to $Cu_{2-x}Se$. Both the Fermi level movement and inner field form the so-called S-scheme heterojunction between $Cu_{2-x}Se$ and $BiVO_4$ [36]. Under illumination, electrons and holes are excited in both materials. In this type of heterojunction, however, the photo-generated electrons in $BiVO_4$ and photo-generated holes in $Cu_{2-x}Se$ will recombine preferentially, due to the band bending and inner field, leaving useful holes in $BiVO_4$. The useful holes possess higher energy level, which can benefit the generation of •OH species. These •OH species can break down long chains of organic matter into small molecules. The above results indicate that loading $Cu_{2-x}Se$ on the surface of $BiVO_4$ can enhance the visible light photocatalytic activity.

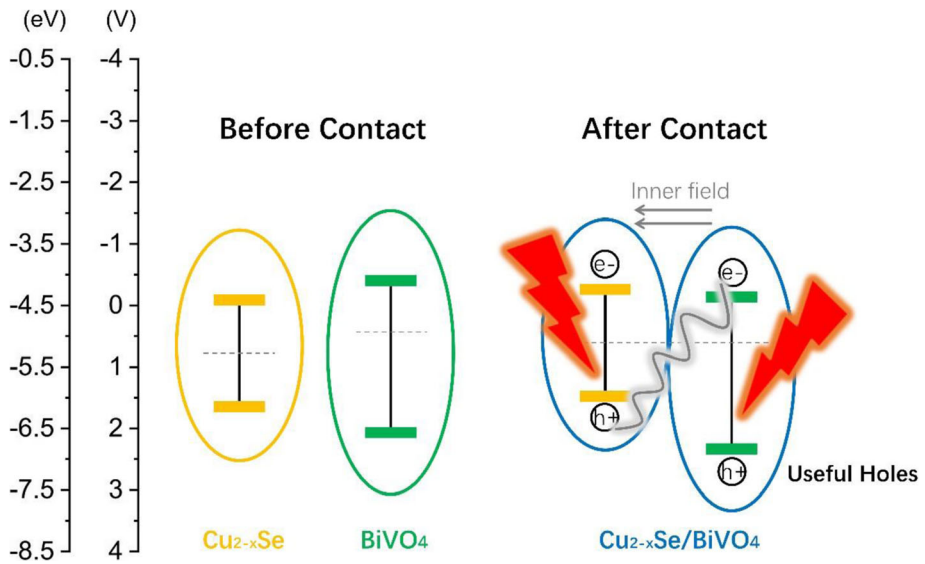

Fig. 7 The schematic diagram of photocatalytic mechanism

Conclusion

In summary, the $Cu_{2-x}Se/BiVO_4$ composites have been successfully prepared and examined for degrading organic pollutions. Experimental data shows that the photocatalytic activity is largely improved after the combination. The photocatalytic efficiency of 3 wt% $Cu_{2-x}Se/BiVO_4$ composite is 15.8 times that of pure $BiVO_4$. Furthermore, after adding low concentration H_2O_2, RhB can be completely degraded within 50 min. The SEM and XPS results confirm the presence of $Cu_{2-x}Se$ in the $Cu_{2-x}Se/BiVO_4$ composites. The results of photoluminescence indicate that the $Cu_{2-x}Se/BiVO_4$ composites have higher electron-hole separation efficiency. The results of EIS indicate that $Cu_{2-x}Se/BiVO_4$ composites have smaller charge transfer resistance and faster interface electron transfer. This work shows that $Cu_{2-x}Se$ is an effective co-catalysis for the development of new composite semiconductor photocatalysts.

Abbreviations

RhB: Rhodamine B; SEM: Scanning electron microscope; XRD: X-ray diffraction

Acknowledgements

We acknowledge financial support from the National Natural Science Foundation of China (Grant No. 51572183 and 51502188).

Availability of Data and Materials

The datasets generated during and/or analyzed during the current study are available from the corresponding author on request.

Authors' Contributions

XL and WZ designed this work. XG and RG performed the experiments. RG analyzed the data. ZL and WZ wrote this paper. All authors read and approved the final manuscript.

Competing Interests

The authors declare that they have no competing interests.

Publisher's Note

Author details

[1]School of Automotive Engineering, Chongqing University, Chongqing 400044, China. [2]School of Material Science and Engineering, Chongqing University, Chongqing 400044, China. [3]Department of Materials, Taizhou University, Taizhou 318000, China.

Received: 14 January 2019 Accepted: 6 March 2019
Published online: 14 March 2019

References

1. Fu JW, Yu JG, Jiang CJ, Cheng B (2018) g-C_3N_4-based heterostructured photocatalysts. Adv Energy Mater 8:1701503
2. Yang HJ, Geng L, Zhang YT, Chang G, Zhang ZL, Liu X, Lei M, He YB (2019) Graphene-templated synthesis of palladium nanoplates as novel electrocatalyst for direct methanol fuel cell. Appl Surf Sci 466:385
3. Xu AJ, Feng SS, Shen SJ, Liu YP, Zhong WW (2018) Enhanced visible light-responsive photocatalytic properties of ag/$BiPbO_2Cl$ nanosheet composites. Nanoscale Res Lett 13:292
4. Wang H, Liu RP, Li YT, Lü XJ, Wang Q, Zhao SQ, Yuan KJ, Cui ZM, Li X, Xin S, Zhang R, Lei M, Lin ZQ (2018) Durable and efficient hollow porous oxide spinel microspheres for oxygen reduction. Joule. 2:337
5. Zhang LY, Gong Y, Wu D, Li Z, Li Q, Zheng L, Chen W (2019) Palladium-cobalt nanodots anchored on graphene: in-situ synthesis, and application as an anode catalyst for direct formic acid fuel cells. Appl Surf Sci 469:305–311
6. Wang X, Cui Y, Li T, Lei M, Li J, Wei Z (2019) Recent advances in the functional 2D photonic and optoelectronic devices. Adv Opt Mater 7: 1801274
7. Pan CS, Xu J, Wang YJ, Li D, Zhu YF (2012) Dramatic activity of $C_3N_4/BiPO_4$ photocatalyst with core/shell structure formed by self-assembly. Adv Funct Mater 22:1518
8. Hu JL, Fan WJ, Ye WQ, Huang CJ, Qiu XQ (2014) Insights into the photosensitivity activity of BiOCl under visible light irradiation. Appl Catal B Environ 158-159:182
9. Fu HB, Pan CS, Yao WQ, Zhu YF (2005) Visible-light-induced degradation of rhodamine B by nanosized Bi_2WO_6. J Phys Chem B 109:22432
10. Liu B, Wang S, Mo Q, Peng L, Cao S, Wang J, Wu C, Li C, Guo J, Liu B, Chen W, Lin Y (2018) Epitaxial MoS_2 nanosheets on nitrogen doped graphite foam as a 3D electrode for highly efficient electrochemical hydrogen evolution. Electrochim Acta 292:407–418
11. Zhong DK, Choi S, Gamelin DR (2011) Near-complete suppression of surface recombination in solar photoelectrolysis by "Co-Pi" catalyst-modified W: $BiVO_4$. J Am Chem Soc 133:18370
12. Yu JQ, Kudo A (2006) Effects of structural variation on the photocatalytic performance of hydrothermally synthesized $BiVO_4$. Adv Funct Mater 16:2163
13. Tokunaga S, Kato H, Kudo A (2001) Selective preparation of monoclinic and tetragonal $BiVO_4$ with Scheelite structure and their photocatalytic properties. Chem Mater 13:4624
14. Wu C, Liu B, Wang J, Su Y, Yan H, Ng C, Li C, Wei J (2018) 3D structured Mo-doped Ni_3S_2 nanosheets as efficient dual-electrocatalyst for overall water splitting. Appl Surf Sci 441:1024–1033
15. Liang C, Tao N, Wang B, Lin S, Lei M (2018) Graphite carbon coated TiN nanoparticles as high durable oxygen reduction reaction catalyst in alkaline electrolyte. Micro Nano Lett 13:1260–1264
16. Tan HL, Amal R, Ng YH (2017) Alternative strategies in improving the photocatalytic and photoelectrochemical activities of visible light-driven $BiVO_4$: a review. J Mater Chem A 5:16498
17. Tan HL, Amal R, Ng YH (2016) Exploring the different roles of particle size in photoelectrochemical and photocatalytic water oxidation on $BiVO_4$. ACS Appl Mater Interfaces 8:28607
18. Guo DY, Su YL, Shi HZ, Li PG, Zhao N, Ye JH, Wang SL, Liu AP, Chen ZW, Li CR, Tang WH (2018) Self-powered ultraviolet photodetector with superhigh photoresponsivity (3.05 A/W) based on the GaN/Sn:Ga_2O_3 pn junction. ACS Nano 12:12827–12835
19. Zheng XW, Hu QT (2009) Facile synthesis and phase control of copper chalcogenides with different morphologies. Appl Phys A Mater Sci Process 94:805
20. Deka S, Genovese A, Zhang Y, Miszta K, Bertoni G, Krahne R, Giannini C, Manna L (2010) Phosphine-free synthesis of p-type copper(I) selenide nanocrystals in hot coordinating solvents. J Am Chem Soc 132:8912
21. Zheng LX, Han SC, Liu H, Yu PP, Fang XS (2016) Hierarchical MoS_2 nanosheet@TiO_2 nanotube array composites with enhanced photocatalytic and photocurrent performances. Small 12:1527
22. Ghosh A, Kulsi C, Banerjee D, Mondal A (2016) Galvanic synthesis of $Cu_{2-x}Se$ thin films and their photocatalytic and thermoelectric properties. Appl Surf Sci 369:525
23. Su JZ, Guo LJ, Bao NZ, Grimes CA (2011) Nanostructured $WO_3/BiVO_4$ heterojunction films for efficient photoelectrochemical water splitting. Nano Lett 11:1928
24. Booshehri AY, Goh SC-K, Hong JD, Jiang RR, Xu R (2014) Effect of depositing silver nanoparticles on $BiVO_4$ in enhancing visible light photocatalytic inactivation of bacteria in water. J Mater Chem A 2:6209
25. Ke D, Peng T, Ma L, Cai P, Jiang P (2008) Photocatalytic water splitting for O_2 production under visible-light irradiation on $BiVO_4$ nanoparticles in different sacrificial reagent solutions. Appl Catal A 350:111
26. Zhong WW, Shen SJ, Feng SS, Lin ZP, Wang ZP, Fang BZ (2018) Facile fabrication of alveolate $Cu_{2-x}Se$ microsheets as a new visible-light photocatalyst for discoloration of rhodamine B. CrystEngComm 20:7851
27. Jiang J, Zhao K, Xiao XY, Zhang LZ (2012) Synthesis and facet-dependent photoreactivity of BiOCl single-crystalline nanosheets. J Am Chem Soc 134:4473
28. Lin S, Bai X, Wang H, Wang H, Song J, Huang K, Wang C, Wang N, Li B, Lei M, Wu H (2017) Roll-to-roll production of transparent silver-nanofiber-network electrodes for flexible electrochromic smart windows. Adv Mater 29:1703238

29. Zhang KF, Liu YX, Deng JG, Xie SH, Zhao XT, Yang J, Han Z, Dai HX (2018) Co-Pd/$BiVO_4$: high-performance photocatalysts for the degradation of phenol under visible light irradiation. Appl Catal B Environ 224:350
30. Guo DY, Shi HZ, Qian YP, Lv M, Li PG, Su YL, Liu Q, Chen K, Wang SL, Cui C, Li CR, Tang WH (2017) Fabrication of beta-Ga_2O_3/ZnO heterojunction for solar-blind deep ultraviolet photodetection. Semicond Sci Technol 32:03LT01
31. Guo D, Liu H, Li P, Wu Z, Wang S, Cui C, Li C, Tang W (2017) Zero-power-consumption solar-blind photodetector based on β-Ga_2O_3/NSTO heterojunction. ACS Appl Mater Interfaces 9:1619–1628
32. Shenasa M, Sainkar S, Lichtman D (1986) XPS study of some selected selenium compounds. J Electron Spectrosc Relat Phenom 40:329
33. Silvester EJ, Grieser F, Sexton BA, Healy TW (1991) Spectroscopic studies on copper sulfide sols. Langmuir 7:2917
34. Jiang ZY, Liu YY, Jing T, Huang BB, Zhang XY, Qin XY, Dai Y, Whangbo M-H (2016) Enhancing the photocatalytic activity of $BiVO_4$ for oxygen evolution by Ce doping: Ce^{3+} ions as hole traps. J Phys Chem C 120:2058
35. Huang QW, Tian SQ, Zeng DW, Wang XX, Song WL, Li YY, Xiao W, Xie CS (2013) Enhanced photocatalytic activity of chemically bonded TiO_2/graphene composites based on the effective interfacial charge transfer through the C-Ti bond. ACS Catal 3:1477
36. Fu J, Xu Q, Lou J, Jiang C, Yu J (2018) Highly porous carbon nitride by supramolecular preassembly of monomers for photocatalytic removal of sulfamethazine under visible light driven. Appl Catal B Environ 243:556